

See discussions, stats, and author profiles for this publication at: <https://www.researchgate.net/publication/38020708>

# Recyclable Molecular Trapping and SERS Detection in Silver-Loaded Agarose Gels with Dynamic Hot Spots

ARTICLE *in* ANALYTICAL CHEMISTRY · OCTOBER 2009

Impact Factor: 5.64 · DOI: 10.1021/ac901333p · Source: PubMed

---

CITATIONS

47

---

READS

63

## 5 AUTHORS, INCLUDING:



**Erwan Faucher**

Valeo

2 PUBLICATIONS 54 CITATIONS

SEE PROFILE



**Ramón A Alvarez-Puebla**

Catalan Institution for Research and Advan...

142 PUBLICATIONS 5,121 CITATIONS

SEE PROFILE



**Mathias Brust**

University of Liverpool

115 PUBLICATIONS 12,263 CITATIONS

SEE PROFILE

# Recyclable Molecular Trapping and SERS Detection in Silver-Loaded Agarose Gels with Dynamic Hot Spots

Paula Aldeanueva-Potel,<sup>†</sup> Erwan Faoucher,<sup>‡</sup> Ramón A. Alvarez-Puebla,<sup>\*,†</sup> Luis M. Liz-Marzán,<sup>†</sup> and Mathias Brust<sup>‡</sup>

Departamento de Química Física and Unidad Asociada CSIC, Universidade de Vigo, 36310 Vigo, Spain, Centre for Nanoscale Science, and Department of Chemistry, University of Liverpool, Crown Street, Liverpool L697ZD, United Kingdom

We describe the design and fabrication of composite agarose gels, highly loaded with silver nanoparticles. Because the gel can collapse upon drying and recover when rehydrated, it can be foreseen as an excellent mechanical molecular trap that additionally gives rise to dynamic hot spots as the network volume decreases and the silver particles get close to each other, thereby generating the high electromagnetic fields that are needed for ultradetection. Additionally, as silver nanoparticles are physically trapped inside the polymer network, analytes can be washed out by dialysis when immersed in a washing solution, so that recycling can be achieved. Finally, the use of SERS for ultradetection of dichlorodiphenyl-trichloroethane (DDT) is reported for the first time, demonstrating the ability of this novel nanocomposite material to reversibly sequester nonconventional SERS analytes.

Development of nanostructured colloids and surfaces with the ability to support localized surface plasmon resonances (LSPR) is turning into a hot field in materials research because of their wide application in different areas such as photonics, medical imaging, drug delivery, catalysis, and ultrasensitive detection via surface-enhanced spectroscopies.<sup>1–3</sup> In the particular case of the latter, and especially in the case of the surface-enhanced Raman scattering (SERS) spectroscopy,<sup>4</sup> the engineering of such optically active materials into advanced assembled composites that will add functionality to the final sensor devices is a key issue.<sup>5–7</sup> Besides

the extraordinary analytical potential of SERS,<sup>8–16</sup> which encompasses the ability for ultrarapid and ultrasensitive detection, down to the single-molecule, while providing all the structural and chemical information of the analyte under study, several shortcomings are still to be resolved. First, at present, SERS cannot be considered as a general analytical technique since registration of enhanced spectra with sufficient quality is basically restricted to molecules carrying functional groups that have sufficient affinity for silver or gold surfaces, which are the most common plasmonic nanostructures.<sup>4,17</sup> Second, the intensity of the SERS signal measured for a given analyte strongly relies on the generation of a high density of so-called hot spots (specific sites where the electric field is largely enhanced)<sup>18–23</sup> on the sensor element. Third, due to the intrinsic nature of the analyte–nanoparticle interactions, most SERS substrates are single-use which hampers their integration in online devices for repetitive, real time monitoring. Currently, a vast effort is being devoted to resolve these drawbacks. For example, extension of the molecular families that may be analyzed has been achieved by using copper nanostruc-

\* Author to whom correspondence should be addressed. E-mail: ramon.alvarez@uvigo.es.

<sup>†</sup> Universidade de Vigo.

<sup>‡</sup> University of Liverpool.

- (1) Daniel, M.-C.; Astruc, D. *Chem. Rev.* **2004**, *104*, 293–346.
- (2) Ghosh, S. K.; Pal, T. *Chem. Rev.* **2007**, *107*, 4797–4862.
- (3) Stewart, M. E.; Anderton, C. R.; Thompson, L. B.; Maria, J.; Gray, S. K.; Rogers, J. A.; Nuzzo, R. G. *Chem. Rev.* **2008**, *108*, 494–521.
- (4) Aroca, R. F. *Surface Enhanced Vibrational Spectroscopy*; Wiley: New York, 2006.
- (5) Strickland, A. D.; Batt, C. A. *Anal. Chem.* **2009**, *81*, 2895–2903.
- (6) Spuch-Calvar, M.; Rodríguez-Lorenzo, L.; Morales, M. P.; Alvarez-Puebla, R. A.; Liz-Marzán, L. M. *J. Phys. Chem. C* **2009**, *113*, 3373–3377.
- (7) Huh, Y. S.; Lowe, A. J.; Strickland, A. D.; Batt, C. A.; Erickson, D. J. *Am. Chem. Soc.* **2009**, *131*, 2208–2213.

- (8) Kneipp, K.; Kneipp, H.; Itzkan, I.; Dasari, R. R.; Feld, M. S. *Chem. Rev.* **1999**, *99*, 2957–2976.
- (9) Rodríguez-Lorenzo, L.; Alvarez-Puebla, R. A.; Pastoriza-Santos, I.; Mazzucco, S.; Stephan, O.; Kociak, M.; Liz-Marzán, L. M.; García de Abajo, F. J. *J. Am. Chem. Soc.* **2009**, *131*, 4616–4618.
- (10) Dieringer, J. A.; Wustholz, K. L.; Masiello, D. J.; Camden, J. P.; Kleinman, S. L.; Schatz, G. C.; Van Duyne, R. P. *J. Am. Chem. Soc.* **2009**, *131*, 849–854.
- (11) Etchegoin, P. G.; Lacharmoise, P. D.; Le Ru, E. C. *Anal. Chem.* **2009**, *81*, 682–688.
- (12) Bell, S. E. J.; Mackle, J. N.; Sirimuthu, N. M. S. *Analyst* **2005**, *130*, 545–549.
- (13) Bell, S. E. J.; Sirimuthu, N. M. S. *Analyst* **2004**, *129*, 1032–1036.
- (14) Bell, S. E. J.; Sirimuthu, N. M. S. *J. Am. Chem. Soc.* **2006**, *128*, 15580–15581.
- (15) Bell, S. E. J.; Sirimuthu, N. M. S. *Chem. Soc. Rev.* **2008**, *37*, 1012–1024.
- (16) Bell, S. E. J.; Spence, S. J. *Analyst* **2001**, *126*, 1–3.
- (17) Alvarez-Puebla, R. A.; Arceo, E.; Goulet, P. J. G.; Garrido, J. J.; Aroca, R. F. *J. Phys. Chem. B* **2005**, *109*, 3787–3792.
- (18) Brus, L. *Acc. Chem. Res.* **2008**, *41*, 1742–1749.
- (19) Camden, J. P.; Dieringer, J. A.; Wang, Y.; Masiello, D. J.; Marks, L. D.; Schatz, G. C.; Van Duyne, R. P. *J. Am. Chem. Soc.* **2008**, *130*, 12616–12617.
- (20) Braun, G.; Pavel, I.; Morrill, A. R.; Seferos, D. S.; Bazan, G. C.; Reich, N. O.; Moskovits, M. *J. Am. Chem. Soc.* **2007**, *129*, 7760–7761.
- (21) Svedberg, F.; Li, Z.; Xu, H.; Kall, M. *Nano Lett.* **2006**, *6*, 2639–2641.
- (22) Le Ru, E. C.; Blackie, E.; Meyer, M.; Etchegoin, P. G. *J. Phys. Chem. C* **2007**, *111*, 13794–13803.
- (23) Ward, D. R.; Grady, N. K.; Levin, C. S.; Halas, N. J.; Wu, Y.; Nordlander, P.; Natelson, D. *Nano Lett.* **2007**, *7*, 1396–1400.

tured materials,<sup>24–26</sup> or by decorating the gold or silver surfaces with molecular systems that are capable of electrostatically,<sup>17,27,28</sup> chemically,<sup>29–32</sup> or mechanically<sup>33,34</sup> trapping analytes that are usually hard to retain. However, nanostructures of first-row metals are unstable and show a strong tendency toward rapid oxidation at open atmosphere or in aqueous solution, thereby losing their plasmonic properties. Regarding surface functionalization, most of the current approaches only partially resolve the problem for certain types of molecules and in most cases the trapping interaction is very strong and thus prevents multiple usage. In the same line, many sensor substrates containing highly efficient hot spots have been recently developed.<sup>35–39</sup> However, again, these substrates can only be used once and may not be able to retain complex molecular systems. In addition, most approaches rely on micro- or nanosized composites, thereby complicating integration within real life devices.

We describe in this paper the design and fabrication of composite agarose gels, densely loaded with silver nanoparticles. Because the gel can collapse upon drying and recover when rehydrated, it can be foreseen as an excellent mechanical molecular trap that additionally gives rise to dynamic hot spots as the network volume decreases and the silver particles get close to each other, thereby generating the huge electromagnetic fields that are needed for ultradetection. Additionally, as silver nanoparticles are physically trapped inside the polymer network, analytes can be washed out by dialysis when immersed in a cleaning solution, so that recycling can be achieved. On the other hand, the bulk dimensions of these composites allow straightforward integration into macro-, micro-, and nanosensor devices. The optical and mechanical trapping properties, as well as the recyclable nature of these systems, were characterized with a number of analytes including thiolated, cationic, anionic, and molecular analytes. Finally, the use of SERS for ultradetection of dichlorodiphenyl-trichloroethane (DDT), an ubiquitous environmental pollutant,<sup>40</sup> which is usually related to diabetes, asthma,

neuropsychological, and psychiatric symptoms and classified as Group 2B carcinogen by the International Agency for Research on Cancer,<sup>41,42</sup> is reported for first time. This demonstrates the ability of this novel nanocomposite material to reversibly sequester nonconventional SERS analytes, such as organochlorine pesticides.

## EXPERIMENTAL METHODS

Unless otherwise stated chemicals were purchased from Sigma Aldrich. Sodium borohydride ( $\text{NaBH}_4$ ) was obtained from BDH, and agarose (molecular grade) from Bioline. All chemicals were used as received. Milli-Q plus 185 water was used in all experiments.

### Synthesis of the Silver-Loaded Agarose Gels (Ag-Agar).

A general protocol for the preparation of metal–nanoparticle-loaded agarose hydrogels is presented elsewhere.<sup>37</sup> Briefly, agarose hydrogels (5.4%w) were prepared by dissolving 285 mg of agarose in 5 mL of water at 90 °C in a glass vial of 20 mm inner diameter followed by sonication until all gas bubbles were removed and storage for at least 1 h at 4 °C. The vial was then carefully destroyed with a small metal hammer (caution!) to isolate the resultant hydrogel, which was rinsed with water and cut with a razor blade into discs of ca. 3.2 mm thickness. For the preparation of silver nanoparticles, a wedge-shaped quarter of an agarose hydrogel disk was immersed in 3 mL of a 500 mM feed solution of  $\text{AgNO}_3$  for 24 h. The hydrogels were then removed from the feed solution, quickly rinsed with water, and immediately transferred to 3 mL of a freshly prepared 500 mM solution of sodium borohydride. After 24 h, the Ag-loaded gels were removed from the sodium borohydride solution and dialyzed in ca. 50 mL of water for 48 h, replacing the water every 12 h. The gels were stored in closed vials under water.

**X-ray Powder Diffraction (XRD).** Data were collected on a Stoe STADI P diffractometer using  $\text{Cu K}\alpha_1$  radiation in transmission foil geometry. Measurements were carried out on ca. 1 mm slices of gel cut with a razor blade. They were held in place between acetate films to prevent shrinkage of the sample by the beam due to dehydration.

**UV–Visible Spectroscopy.** Solid-state spectra were recorded with a Perkin-Elmer Lambda 650 S UV/vis spectrometer equipped with a Labsphere integrating sphere over the spectral range 190–900 nm (6.53–1.38 eV) using  $\text{BaSO}_4$  reflectance standards. Samples were prepared by compressing a small piece of gel between two glass slides. A sample of unloaded gel was used as a reference.

**Transmission Electron Microscopy (TEM).** Before the gels were embedded in epoxy resin, they were dehydrated in a graded series of ethanol solutions (30, 60, 70, 90, and 100%) for 30 min at each concentration and then infiltrated by a graded series of epoxy resin in absolute ethanol (proportion of resin was 1/4, 1/2, and 3/4 of the total volume) each step for 1 h. After being embedded in the pure resin, it was polymerized at 60 °C for one week. This unusually slow step was necessary to avoid irreversible sticking of the sample to the diamond blade during the subsequent cutting process. Ultrathin sections (60 nm) were cut using a LKB

- (24) Pastoriza-Santos, I.; Sánchez-Iglesias, A.; Rodríguez-González, B.; Liz-Marzán, L. M. *Small* **2009**, *5*, 440–443.
- (25) Anema, J. R.; Brolo, A. G.; Marthandam, P.; Gordon, R. J. *Phys. Chem. C* **2008**, *112*, 17051–17055.
- (26) Kudelski, A. *Langmuir* **2003**, *19*, 3805–3813.
- (27) Alvarez-Puebla, R. A.; Aroca, R. F. *Anal. Chem.* **2009**, *81*, 2280–2285.
- (28) Tan, S.; Erol, M.; Sukhishvili, S.; Du, H. *Langmuir* **2008**, *24*, 4765–4771.
- (29) Guerrini, L.; Garcia-Ramos, J. V.; Domingo, C.; Sanchez-Cortes, S. *Langmuir* **2006**, *22*, 10924–10926.
- (30) Guerrini, L.; Garcia-Ramos, J. V.; Domingo, C. n.; Sanchez-Cortes, S. *Anal. Chem.* **2009**, *81*, 953–960.
- (31) Guerrini, L.; Garcia-Ramos, J. V.; Domingo, C. n.; Sanchez-Cortes, S. *Anal. Chem.* **2009**, *81*, 1418–1425.
- (32) Bantz, K. C.; Haynes, C. L. *Vib. Spectrosc.* **2009**, *50*, 29–35.
- (33) Alvarez-Puebla, R. A.; Contreras-Caceres, R.; Pastoriza-Santos, I.; Perez-Juste, J.; Liz-Marzán, L. M. *Angew. Chem., Int. Ed.* **2009**, *48*, 138–143.
- (34) Abalde-Cela, S.; Ho, S.; Rodríguez-González, B.; Correa-Duarte, Miguel, A.; Álvarez-Puebla, Ramón, A.; Liz-Marzán, Luis, M.; Kotov, Nicholas, A. *Angew. Chem., Int. Ed.* **2009**, *48*, 5326–5329.
- (35) Le, F.; Brandl, D. W.; Urzhumov, Y. A.; Wang, H.; Kundu, J.; Halas, N. J.; Aizpurua, J.; Nordlander, P. *ACS Nano* **2008**, *2*, 707–718.
- (36) Kneipp, J.; Li, X.; Sherwood, M.; Panne, U.; Kneipp, H.; Stockman, M. I.; Kneipp, K. *Anal. Chem.* **2008**, *80*, 4247–4251.
- (37) Faucher, E.; Nativo, P.; Black, K.; Claridge, J. B.; Gass, M.; Romani, S.; Bleloch, A. L.; Brust, M. *Chem. Commun.*, in press, DOI: 10.1039/B915787E.
- (38) Park, Y.-K.; Yoo, S.-H.; Park, S. *Langmuir* **2008**, *24*, 4370–4375.
- (39) Lee, S. J.; Morrill, A. R.; Moskovits, M. *J. Am. Chem. Soc.* **2006**, *128*, 2200–2201.
- (40) Turusov, V.; Rakitsky, V.; Tomatis, L. *Environ. Health Perspect.* **2002**, *110*, 125–128.

- (41) Ahlborg, U. G.; Lipworth, L.; Titus-Ernstoff, L.; Hsieh, C. C.; Hanberg, A.; Baron, J.; Trichopoulos, D.; Adami, H. O. *Crit. Rev. Toxicol.* **1995**, *25*, 463–531.
- (42) Longnecker, M. P.; Rogan, W. J.; Lucier, G. *Annu. Rev. Public Health* **1997**, *18*, 211–244.

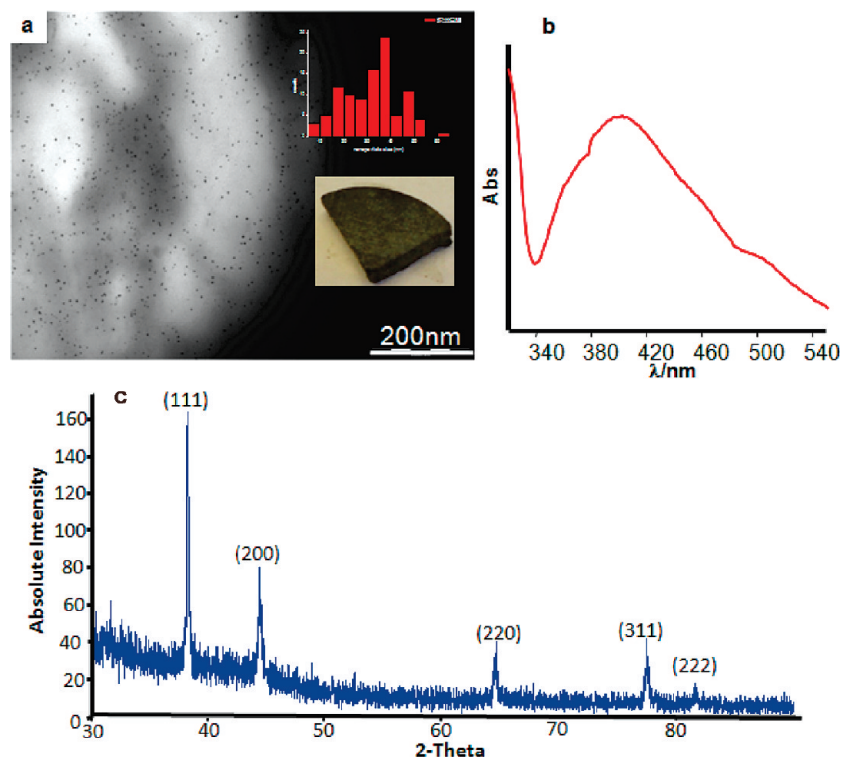


**Figure 1.** (A) Cross-sectional TEM image of the Ag-Agar gel (inset shows an optical picture of the bulk polymer). (B) UV-vis spectrum and (C) X-ray diffraction pattern of the Ag-Agar gel.

ultramicrotome. The sections were placed on a carbon-coated copper grid and dried at room temperature. TEM images were obtained using a 120 kV FEI technai Spirit TEM.

**SERS.** The inelastic scattered radiation was collected with a Renishaw Invia Reflex system equipped with Peltier charge-coupled device (CCD) detectors and a Leica confocal microscope. The spectrograph uses high resolution gratings with additional band-pass filter optics. Samples were excited with four different laser lines at 532 (Nd:Yag), 633 (He-Ne), and 785 and 830 nm (diode). The corresponding laser line was focused onto the sample in backscattering geometry using a 50 $\times$  objective (n.a. 0.75) providing scattering areas of ca. 1  $\mu\text{m}^2$ .

The SERS optical activity of the Ag-Agar composites was tested with 1-naphthalenethiol (1NAT, Acros Organics), a well-studied nonresonant SERS probe. Samples were prepared by immersing the polymer into 1NAT  $10^{-5}$  M aqueous solution for 2 h. SERS spectra were collected on the wet and dried gel with each of the laser lines. Optical enhancing homogeneity of the Ag-Agar was studied by using the Renishaw StreamLine accessory with the 785 nm laser line.

For dichlorodiphenyl-trichloroethane (DDT), the analysis was carried out by immersing the Ag-Agar in DDT aqueous solutions of different concentration (between  $10^{-4}$  and  $10^{-8}$  M) prepared from DDT  $10^{-3}$  M stock solution in ethanol for 2 h. After being dried, the surfaces were studied with the 785 nm laser line.

Reversibility as a function of the analyte charge was studied by immersing the Ag-loaded agarose gel, either in crystal violet  $10^{-6}$  M (CV, cationic probe), 2-naphthoic acid  $10^{-5}$  M (NCOOH, anionic probe), or DDT  $10^{-5}$  M (neutral probe) for 2 h. Samples were then studied with either 633 or 785 nm laser lines and immersed in a washing 1% citrate aqueous solution for 2 h, CV and NCOOH, and an ethanol:water (1:1) mixture. This

process was repeated three times for each sample to ensure reproducibility.

## RESULTS AND DISCUSSION

A general structural model for agarose gels loaded with in situ prepared metal nanoparticles based on high resolution imaging is presented in detail elsewhere.<sup>37</sup> In summary, metal nanoparticles of two size ranges are usually obtained: (i) large, 8 to 60 nm, particles dispersed in the water phase of the gel, and (ii) small, 0–5 nm, clusters and nanoparticles decorating the gel's polymeric framework. This is also the case for Ag as shown in the TEM image of a section of the loaded gel in Figure 1a. Here, the larger particles as well as aggregates thereof are resolved as irregularly shaped black specks, while the electron dense coating of the gel network with small clusters appears as a homogeneous gray cloud. More highly resolved electron microscopy images are difficult to obtain with the combination of material and sample preparation technique chosen here and are not subject of the present study. The suggested model is further supported by XRD (Figure 1b), which clearly shows the presence of *fcc* Ag nanoparticles, the approximate average size of which can be estimated as 33 nm by Scherrer line broadening analysis.<sup>38</sup> The material appears yellow to dark brown depending on thickness, which is consistent with the presence of Ag nanoparticles with a plasmon absorption band around 420 nm. The UV-vis spectrum shown in Figure 1c is in agreement with this observation, although the plasmon band is unusually broad and slightly blue-shifted. This could be due to scattering by the gel network, which scales as  $\lambda^{-4}$  and would enhance the total extinction at low wavelengths.

Consistent with the low SERS cross-section of polysaccharides,<sup>4</sup> the background SERS spectra of the dry, unloaded (with no



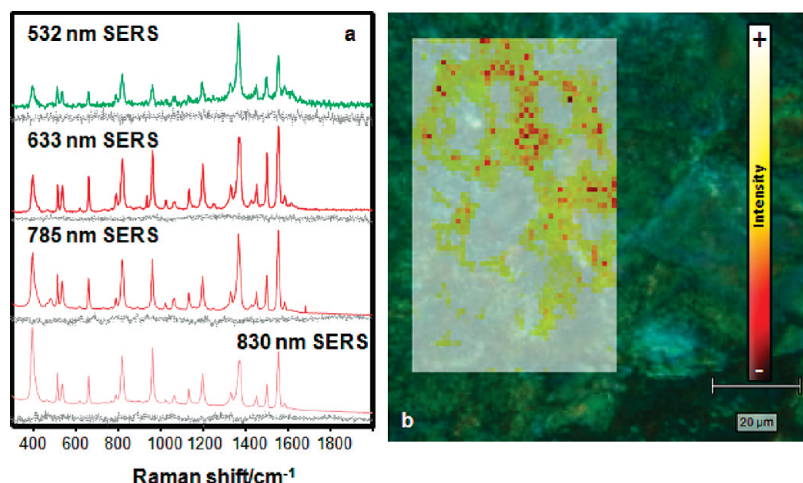


**Figure 2.** (A) SERS spectra of the dry Ag-Agar gel with 1NAT (colored spectra) and without the analyte (gray spectra). (B) StreamLine map of the Ag-Agar gel with 1NAT (785 nm) composed of 2639 spectra with spatial resolution of ca. 1  $\mu\text{m}^2$ .

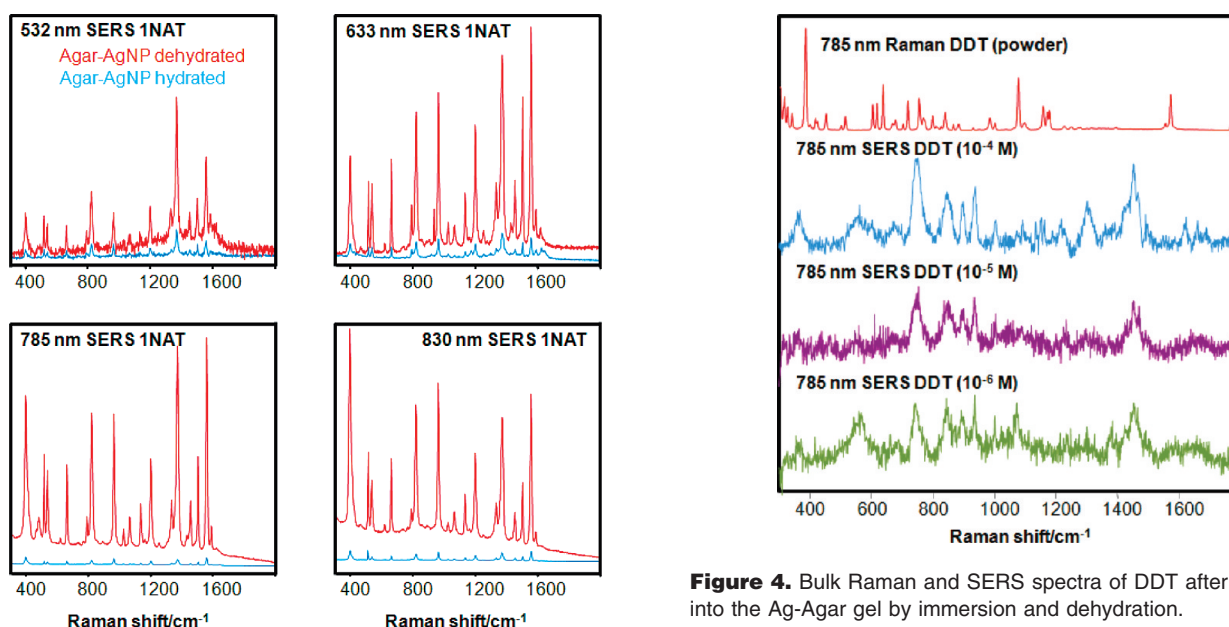


**Figure 3.** SERS spectra of 1NAT in Ag-Agar before and after air-drying the gel for different excitation laser lines (532, 633, 785, and 830 nm).

analyte) Ag-Agar gels (gray lines in Figure 2A) present a very clean spectral window from the visible (532 nm) to the near-IR (830 nm). In contrast, upon immersion of the gel in an aqueous solution of 1-naphtalenethiol (1NAT) and subsequent air-drying, the SERS spectra (colored lines in Figure 2A) show well-defined bands with high intensity, which are characteristic of 1NAT: ring stretching (1553, 1503, and 1368  $\text{cm}^{-1}$ ), CH bending (1197  $\text{cm}^{-1}$ ), ring breathing (968 and 822  $\text{cm}^{-1}$ ), ring deformation (792, 664, 539, and 517  $\text{cm}^{-1}$ ), and CS stretching (389  $\text{cm}^{-1}$ ),<sup>43</sup> regardless of the laser line used and even using very low laser power at the sample ( $\sim 1 \mu\text{W}$ ). SERS mapping (Figure 2B) clearly shows that the SERS enhancing ability of the Ag-loaded gel is homogeneous through the entire surface, which reveals that this is an extremely clean and efficient substrate for SERS, allowing ultra-sensitive detection in a wide spectral window of excitation

**Figure 4.** Bulk Raman and SERS spectra of DDT after trapping it into the Ag-Agar gel by immersion and dehydration.

wavelengths (from the green to the near-IR). The high intensity provided by these materials is related to the generation of a high density of hot spots when the gel collapses upon dehydration. The consequent volume reduction of the material (ca. 12-fold, as compared with its hydrated form) drives the embedded colloidal silver nanoparticles close to each other, thus promoting the interaction between their respective electromagnetic fields and therefore further increasing the enhanced Raman signal.

For demonstration of this concept of dynamic hot spots, SERS spectra of 1NAT in Ag-Agar were acquired using all available excitation laser lines, both before and after dehydration. Figure 3 shows the substantial increase of the signal in all cases, though in a more pronounced manner as the laser energy is decreased (toward the IR), ranging from barely 10-fold in the case of the green line (532 nm) to over 100 fold in the case of the NIR lines (785 and 830 nm). This observation can be easily explained considering that the electromagnetic coupling between two or more metallic nanoparticles has been consistently reported to red-shift the corresponding LSPR,<sup>44</sup> so that the overlap between LSPR

(43) Alvarez-Puebla, R. A.; Dos Santos, D. S., Jr.; Aroca, R. F. *Analyst* **2004**, *129*, 1251–1256.

(44) Jain, P. K.; Huang, W.; El-Sayed, M. A. *Nano Lett.* **2007**, *7*, 2080–2088.

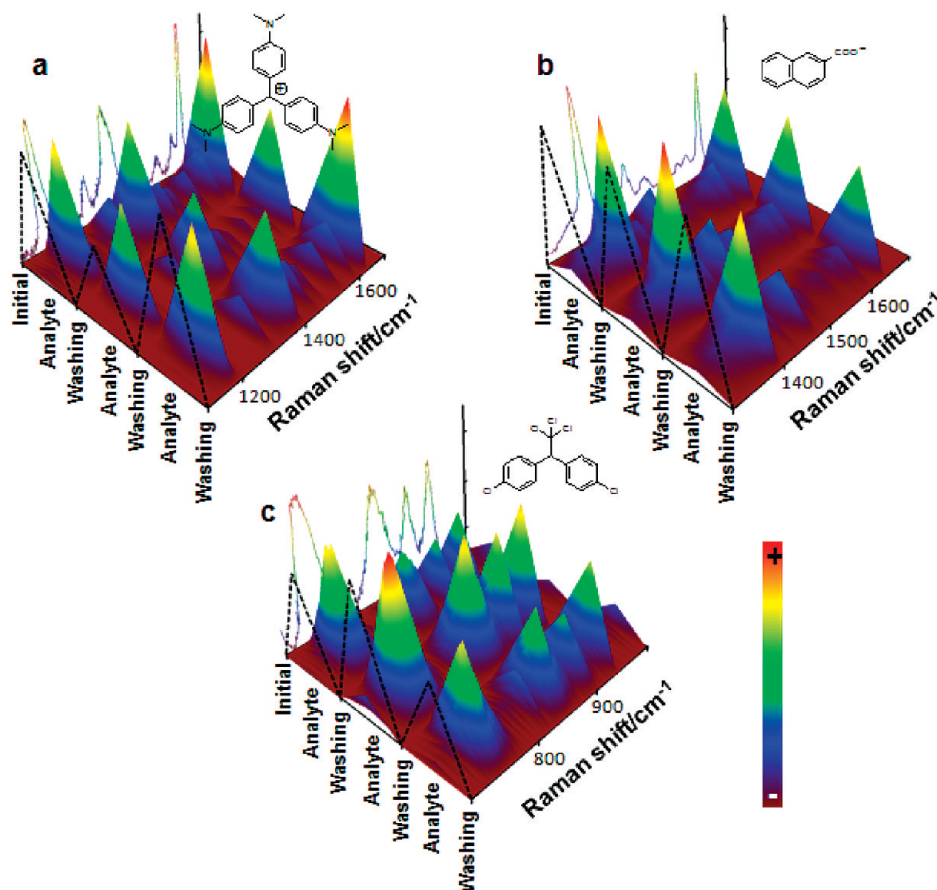


**Figure 5.** Reversible SERS behavior of Ag-Agar gel after immersing the polymer into solutions containing (a) crystal violet  $10^{-6}$  M, (b) 2-naphthoic acid  $10^{-5}$  M, and (c) DDT  $10^{-5}$  M, after washing with 1% citrate aqueous solution, CV and NCOOH, and water-ethanol mixture (1:1), DDT.

and laser line is improved for longer wavelength excitations. This results in an increase of the enhancement of the SERS signal when excited using lower energy lasers, as predicted by the electromagnetic mechanism because of the better laser-plasmon overlap, in a fashion similar to that of surface-enhanced Raman excitation spectroscopy.<sup>45–47</sup>

The clear advantages of this new system, i.e., its superior optical enhancing properties together with the reversible dehydration and rehydration ability, for dynamic generation of optical hot spots and molecular trapping, were demonstrated through a series of experiments. The trapping efficiency of Ag-Agar was tested using a small and relevant contaminant, the organochlorine DDT. The SERS spectrum of this widespread pesticide has not been reported so far, because it cannot be adsorbed onto metallic surfaces in general, and on silver or gold in particular. Nevertheless, by immersing Ag-Agar gels in DDT aqueous solutions of various concentrations ( $10^{-4}$ – $10^{-8}$  M) and subsequently collapsing the gel by dehydration, it has been possible to obtain a well resolved Raman-enhanced vibrational pattern of the target molecule (Figure 4). The spectrum was found to be fully reproducible and is characterized by the ring stretchings (1491, 1467, 1451, and 1428  $\text{cm}^{-1}$ ), aliphatic CC stretching (1297  $\text{cm}^{-1}$ ), CH bending (1091  $\text{cm}^{-1}$ ), ring breathing (1001  $\text{cm}^{-1}$ ), ring

deformation (935  $\text{cm}^{-1}$ ), CH twisting (899 and 848  $\text{cm}^{-1}$ ), CH wagging (745  $\text{cm}^{-1}$ ), and CCl stretchings (685 and 554  $\text{cm}^{-1}$ ). Notably, the vibrational pattern of DDT could be unequivocally recognized, even for concentrations down to the micromolar regime. Although this may not seem an extremely high sensitivity, as compared with other analytical techniques,<sup>48–50</sup> it should be taken into account that SERS spectra can be acquired in very short times and with basically no need for prior sample treatment.

Finally, the reversibility of the Ag-Agar gels was studied for a variety of molecular probes. Figure 5 shows the results for a cation (crystal violet, CV), an anion (2-naphthoic acid, NCOOH), and a neutral molecular species, DDT. In all cases, the gel was first immersed in the solution containing the corresponding analyte, characterized by SERS, and immersed in a washing aqueous solution of 1 wt % sodium citrate, and the SERS spectra were measured again. This process was repeated three times to ensure the full reusability of this sensor platform.

Remarkably, for each of these different analytes, the characteristic vibrational patterns could be clearly identified when the analyte was present but were completely removed upon washing.

(45) Alvarez-Puebla, R. A.; Ross, D. J.; Nazri, G.-A.; Aroca, R. F. *Langmuir* **2005**, *21*, 10504–10508.

(46) Haynes, C. L.; Van Duyne, R. P. *J. Phys. Chem. B* **2003**, *107*, 7426–7433.

(47) McFarland, A. D.; Young, M. A.; Dieringer, J. A.; Van Duyne, R. P. *J. Phys. Chem. B* **2005**, *109*, 11279–11285.

(48) Graham, A. L.; Carlson, C. A.; Edmiston, P. L. *Anal. Chem.* **2002**, *74*, 458–467.

(49) Alvarez, M.; Calle, A.; Tamayo, J.; Lechuga, L. M.; Abad, A.; Montoya, A. *Biosens. Bioelectron.* **2003**, *18*, 649–653.

(50) Moreno Frias, M.; Garrido Frenich, A.; Martinez Vidal, J. L.; Mateu Sanchez, M.; Olea, F.; Olea, N. *J. Chromatogr. B: Anal. Technol. Biomed. Sci. Appl.* **2001**, *760*, 1–15.

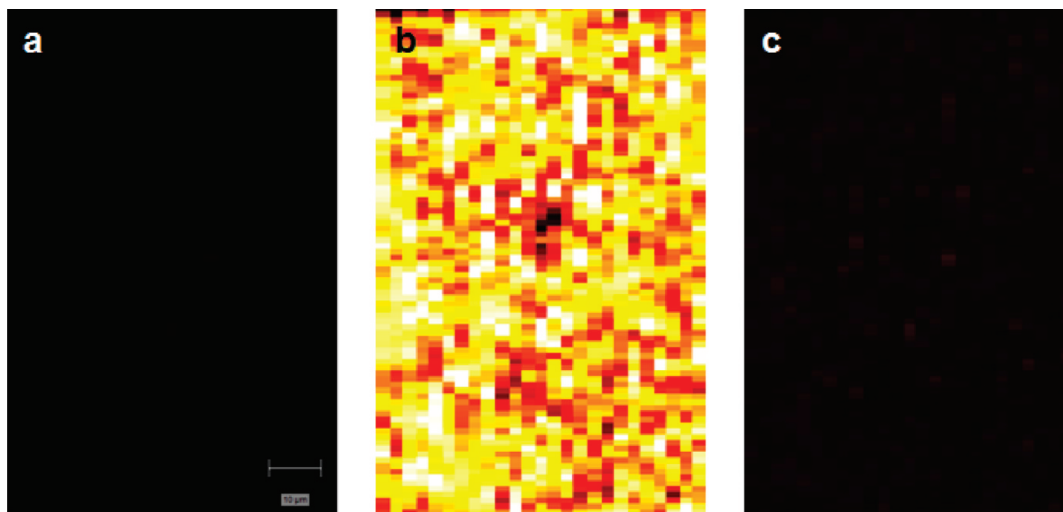


**Figure 6.** SERS maps of the Ag-Agar gel before (a) and after (b) CV addition, as well as after washing with 1% trisodium citrate in water (c).

To ensure that the effect is not an artifact due to the occasional measurement of hot spots, extended mapping was carried out on the blank polymer, after addition of the analyte and after washing (Figure 6). For charged species, it is very likely that sodium and citrate ions compete for the retention sites of the analyte on the nanoparticles, thus displacing it because of their much higher concentration and thereby cleaning the sensor. When the analyte was again in contact with the gel, it was retained, giving rise to signals of similar intensity. In the case of DDT, although the same washing process was followed, it was observed that the low affinity of this molecule toward metallic surfaces makes the citrate solution unnecessary, rendering the sensor ready for reutilization after simply washing with water. These results further demonstrate the trapping properties of the gel, together with its reversibility for a wide variety of substances with different chemical properties, within a material that is capable of generating dynamic hot spots with extremely high enhancing activity, which is comparable to that of aggregated silver colloids.

## CONCLUSIONS

In summary, we devised a novel material that benefits from unique characteristics offering at the same time reversible sequestering properties and high SERS intensity, which allows for fast ultradetection of a wide range of molecular systems, while smoothing the way toward the generation of online sensors capable to monitor continuous flows in real time.

## ACKNOWLEDGMENT

P.A.-P. and E.F. have contributed equally to the present work. R.A.A.-P. acknowledges the RyC (MEC, Spain) program. This work has been funded by the Spanish Ministerio de Ciencia e Innovación (Grants MAT2007-62696 and MAT2008-05755, Consolider Ingenio 2010-CSD2006-12) and the Xunta de Galicia (Grants PGIDIT06TMT31402PR, 08TMT008314PR). E.F. acknowledges financial support via an EPSRC quota Ph.D. studentship.

Received for review June 19, 2009. Accepted September 2, 2009.

AC901333P